X-621-68-469
PREPRINT

DOCUMENTATION OF EXPLORER 32 ELECTRON TEMPERATURE MEASUREMENTS USED IN COMPARISONS WITH BACKSCATTER MEASUREMENTS AT JICAMARCA

L.H. BRACE

P.L. DYSON

NOVEMBER 1968

GODDARD SPACE FLIGHT CENTER
GREENBELT, MARYLAND

X-621-68-469

DOCUMENTATION OF EXPLORER 32 ELECTRON TEMPERATURE MEASUREMENTS USED IN COMPARISONS WITH BACKSCATTER MEASUREMENTS AT JICAMARCA

L. H. Brace and P. L. Dyson*

November 1968

GODDARD SPACE FLIGHT CENTER
Greenbelt, Maryland

*NRC-NASA Resident Research Associate

DOCUMENTATION OF EXPLORER 32 ELECTRON TEMPERATURE MEASUREMENTS USED IN COMPARISONS WITH BACKSCATTER MEASUREMENTS AT JICAMARCA

L. H. Brace and P. L. Dyson*

ABSTRACT

A series of Explorer 32 satellite passes over Jicamarca have provided direct measurements of electron temperature that disagree significantly with those derived from radar backscatter data. In this paper we (1) briefly describe the Explorer 32 electrostatic probe experiments, (2) present the experimental data from which the satellite values of electron temperature were derived, (3) outline the analysis procedure, and (4) discuss the known sources of random and systematic error.

We conclude that the excellent quality of the data, the linearity of the $\log_e I_e$ plots over nearly two decades of electron current, and the agreement between the values derived from the two independent probe experiments make it difficult to understand how the probe-derived temperatures could be in error by a factor large enough to explain the disagreement with backscatter data.

*NRC-NASA Resident Research Associate

CONTENTS

DOCUMENTATION OF EXPLORER 32 ELECTRON TEMPERATURE MEASUREMENTS USED IN COMPARISONS WITH BACKSCATTER MEASUREMENTS AT JICAMARCA

INTRODUCTION

The second Atmospheric Explorer, Explorer 32, was placed in orbit on May 25, 1966 with an orbital inclination of 64.5° and perigee and apogee altitudes of 270 kilometers and 2700 kilometers, respectively. Among the instruments carried by this satellite were two cylindrical electrostatic probe experiments which were employed to measure the electron temperature, T_e, and concentration, N_e.

Because of the complementary nature of satellite and radar backscatter measurements of the ionosphere, a program of simultaneous operation was begun in the summer of 1966 with the cooperation of scientists at the Jicamarca radar facility near Lima, Peru, where a STADAN station was available for interrogating the satellite. The first task was to compare the electron temperature measurements taken when the satellite was nearest Jicamarca, this to be followed by studies in which the satellite measurements would provide information about the latitudinal behavior of the ionosphere while the radar provided the vertical structure and its diurnal variations.

Unfortunately the initial comparisons of T_e revealed that the probe-derived values were about a factor of 1.7 greater than the radar-derived values (Hanson, et al., 1968). Table I summarizes that intercomparison data. As can be seen, the difference was apparently independent of time of day or altitude. No explanation of this discrepancy has been offered and none is offered here.

However, in view of the difference between probe and radar measurements of T_e, we have written this report to document the probe method and to present the data which are the basis for these particular comparisons. We hope that these data will be examined critically for any conceivable error.

Table 1

Pass No.	Date (1966)	Altitude (km)	LT (hours)	Electron Temperature (°K)		
				Probe 1	Probe 2	Radar
LIMA 934	8 Aug.	571	1600	2075	2000	1150
LIMA 1020	15 Aug.	540	1435	1970	2075	1150
LIMA 1328	9 Sept.	488	0903	1800	1870	1100
LIMA 1747	13 Oct.	422	0220	1070	1250	740
LIMA 2141	13 Nov.	366	1945	1610	1585	875

THE PROBE METHOD

Cylindrical electrostatic probes of the type employed on Explorer 32 were first used in the ionosphere in a series of rocket flights beginning in 1961 (Spencer, Brace and Carignan, 1962) (Spencer, et al., 1965). The method was extended to satellite use in April 1963 when the first Atmospheric Explorer satellite, Explorer 17, was launched (Brace, Spencer and Dalgarno, 1965). Thereafter cylindrical probes were employed on the TIROS-7 satellite (Reddy, Brace, Findlay, 1967), the Explorers 22 and 27 (Brace and Reddy, 1965) (Brace, Reddy and Mayr, 1967) and the ISIS-X satellites, Explorer 31 and Alouette-II, (Findlay and Brace, 1968) (Brace and Findlay, 1968).

Theory

The theory and implementation of the cylindrical probe method is covered in the above referenced papers, therefore we will only briefly review those aspects which are special to the Explorer 32 application or are needed to follow the progression from raw telemetry data to the derived value of T_e.

When a conductor is placed in a plasma and its potential is varied, the amplitude of the volt-ampere characteristic depends directly upon the electron concentration while the shape of the characteristic depends upon the thermal properties of the plasma. The equation which describes the electron current to a negative collector was given by Mott-Smith and Langmuir (1926).

$$I_e = A N_e e \left(kT_e/2\pi m_e\right)^{1/2} e^{-eV/kT_e} \tag{1}$$

where

A = probe surface area

N_e = electron concentration

T_e = electron temperature

m_e = electron mass

e = electron charge

k = Boltzmann's constant

V = voltage of probe relative to the plasma

Solving (1), T_e is given by

$$T_e = \frac{e}{k} \frac{dV}{d \ell n I_e} . \tag{2}$$

Thus the electron temperature in the plasma can be derived from the change in $\ell n\, I_e$ which occurs in response to a known change in the probe voltage, dV.

The equation which describes the electron current to a positive collector depends upon the geometry of the collector. For the orbital-motion-limited cylinder employed here, the electron current is given by

$$I_e = A N_e e \left(kT_e / 2\pi m_e\right)^{1/2} \cdot \frac{2}{\pi^{1/2}} \left(1 + eV/kT_e\right)^{1/2}, \qquad eV/kT_e > 2 . \quad (3)$$

This has been shown to reduce to

$$I_e = \frac{A N_e e}{\pi} \left(2eV/m_e\right)^{1/2}, \qquad eV/kT_e >> 1 . \quad (4)$$

This equation is convenient when a large amount of data are to be analyzed for N_e, because the value of T_e need not be determined first.

Experiment

Figure 1 shows the manner in which the various sensors on Explorer 32 were mounted on the satellite surface. The spacecraft was a vacuum-tight spherical shell made of stainless steel. An attitude control system was operated occasionally to maintain the spin axis of the satellite nearly normal to the orbital plane. Most of the sensors were mounted on the equator of the sphere to take advantage of the full range of angles of attack experienced there as the satellite rotated at about 30 revolutions per minute.

Two entirely independent probes and electronic systems were employed to provide redundancy, greater spatial resolution and a wider dynamic range. The probes were mounted at the equator on opposite sides of the spacecraft. Each collector was 23 cm long and 0.06 cm in diameter, and each extended from the end of a concentric guard electrode of similar length. Thus the tip of the probe extended about 46 cm into the plasma surrounding the spacecraft. Both the guards and collectors were made of stainless steel as on previous rocket and satellite applications of this method.

Figure 2 shows the electrical arrangement employed to sweep the collector and guard voltage (V_a) and measure the collector current. The data sampling

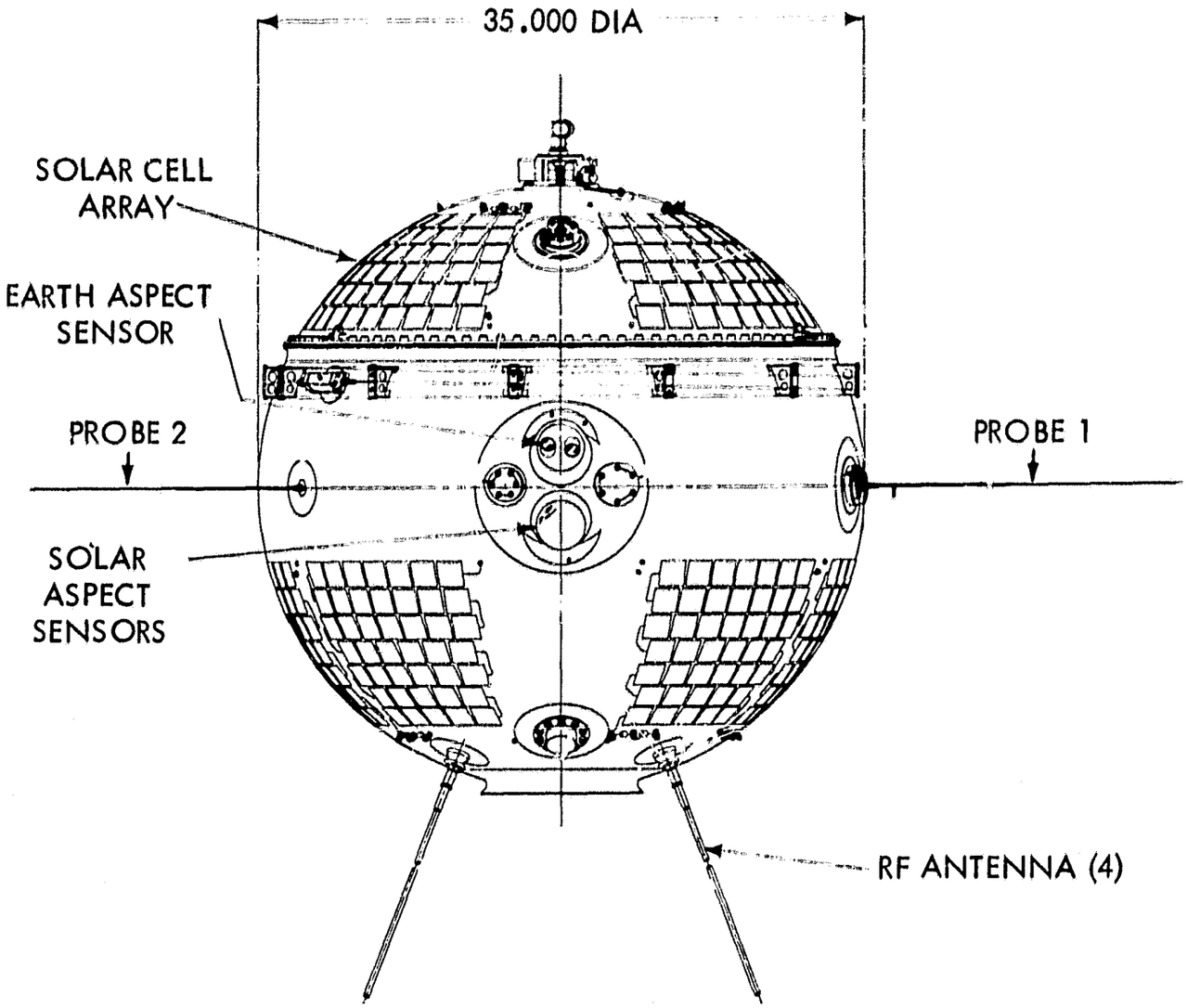

Figure 1. Explorer 32 Spacecraft. Two independent cylindrical probes were mounted on the equator of the spinning satellite.

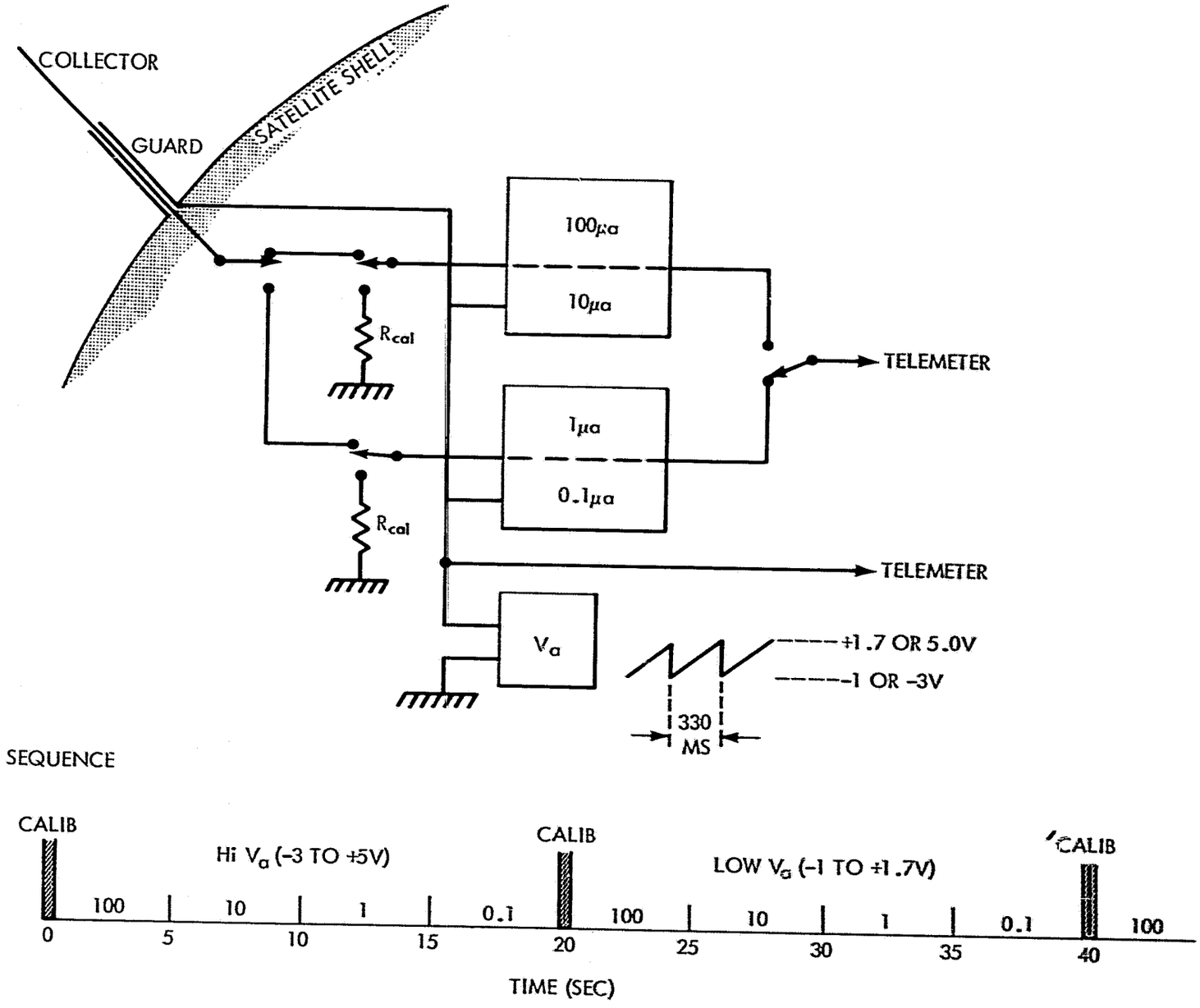

Figure 2. The electrical arrangement and timing sequence of probe system number 2. Probe 1 system was identical except that the current sensitivities were greater (50, 5, 0.5, 0.05 μa, respectively).

sequence is shown at the bottom of the figure. Four linear current ranges and two sawtooth amplitudes were employed in sequence to provide the necessary current and voltage resolution over the wide range of electron concentration and temperature encountered along the orbit. The sawtooth voltage sweep was repeated at 330 millisecond intervals throughout each 4-minute turn-on of the satellite. The current range was stepped at 5 second intervals and the voltage amplitude was changed at the end of each range sequence. Thus about 15 volt-ampere curves were obtained in each of the four current ranges.

Figures 3 and 4 show a complete cycle of data from one probe which further illustrates the sampling sequence and the nature of the experimental data. These curves were traced from a computer plot of raw telemetry data, and they are particularly valuable for illustrating the wake effects. When the probe rotates through the wake of the satellite, the electron and ion currents are greatly reduced in amplitude, and the shape of the characteristics is often badly distorted as are the curves labelled W in the figures. These effects are evident at two second intervals (the spin period) and either one or two curves are affected, depending upon where they occur in the spin cycle. Similar wake effects are observed in both the ion and electron currents, although ion currents are only resolved on the more sensitive current ranges. The depth of the wake varies greatly from pass to pass since it depends largely upon the ion mass and temperature.

Telemetry Resolution

The amplitudes and period of the sawtooth (V_a) represented a compromise between voltage resolution requirements and spin period limitations imposed by the other experiments on Explorer 32. The need for at least 5 or 6 sweeps per spin and the availability of 170 telemetry samples per second made it necessary to employ a low sweep amplitude for T_e and a high sweep amplitude for N_e. The voltage resolution attained in this way is demonstrated in Figures 5 and 6. Figure 5 illustrates a single volt-ampere characteristic taken on high V_a with a current range which resolves the entire characteristic. The amplitude of the electron saturation region, visible to the right of the plasma potential, is employed for deriving N_e. The electron retardation region, visible at the left, is not well resolved on this voltage and current range.

When T_e is to be derived, a more sensitive range is employed which resolves only the electron retardation region as illustrated in Figure 6. This figure also illustrates the voltage resolution available on low V_a at moderate temperatures. The 50 millivolt sampling increment is adequate for resolving temperatures well below 500°K, such as are often seen in the E-region on rocket flights of this instrument.

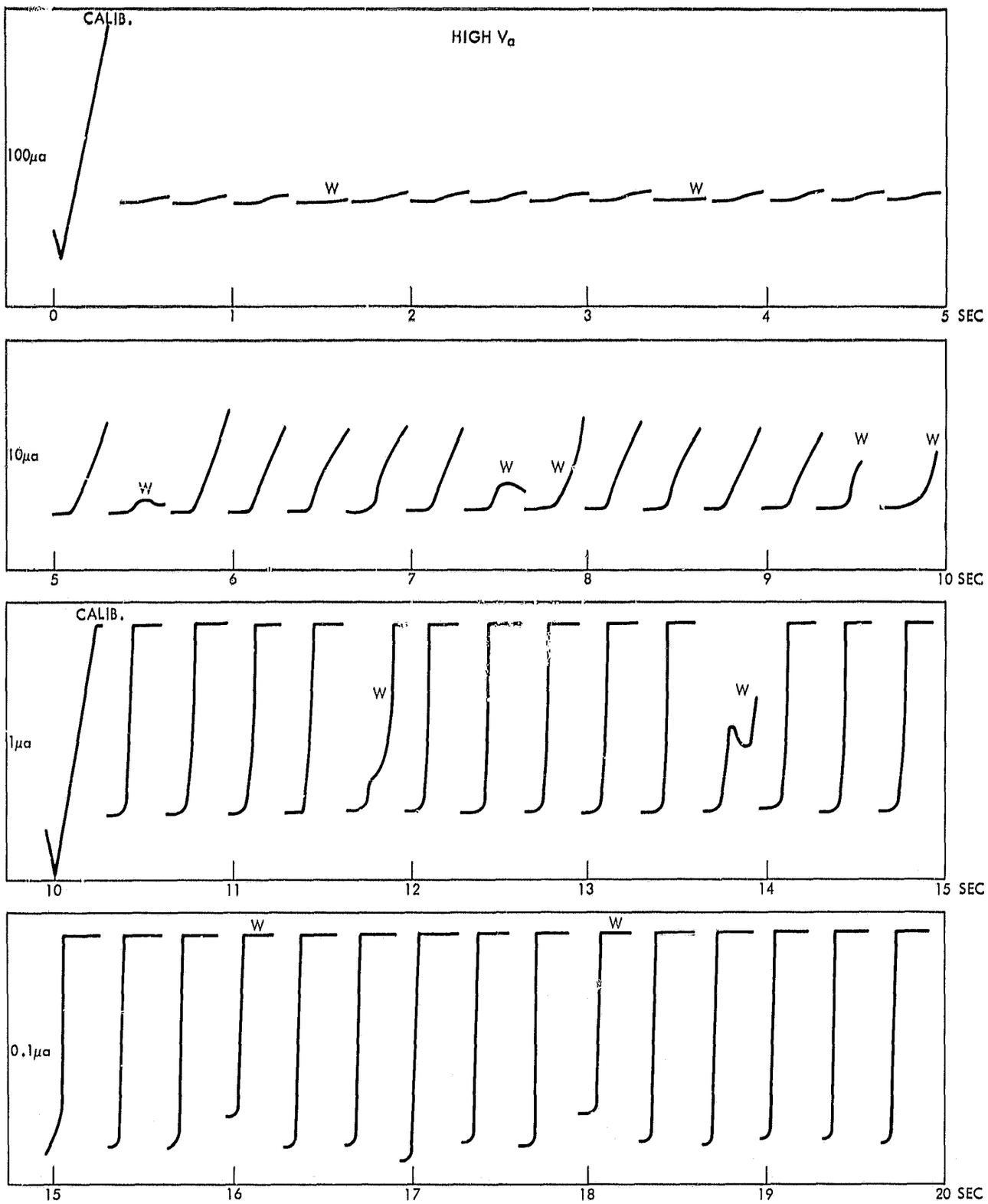

Figure 3. Analog tracing of data from a high V_a sequence from probe 2. Approximately 15 volt-ampere curves are taken on each current range. The current range is sequenced at 5-second intervals. Wake effects (w) appear at 2-second intervals as the probe rotates into the spacecraft wake.

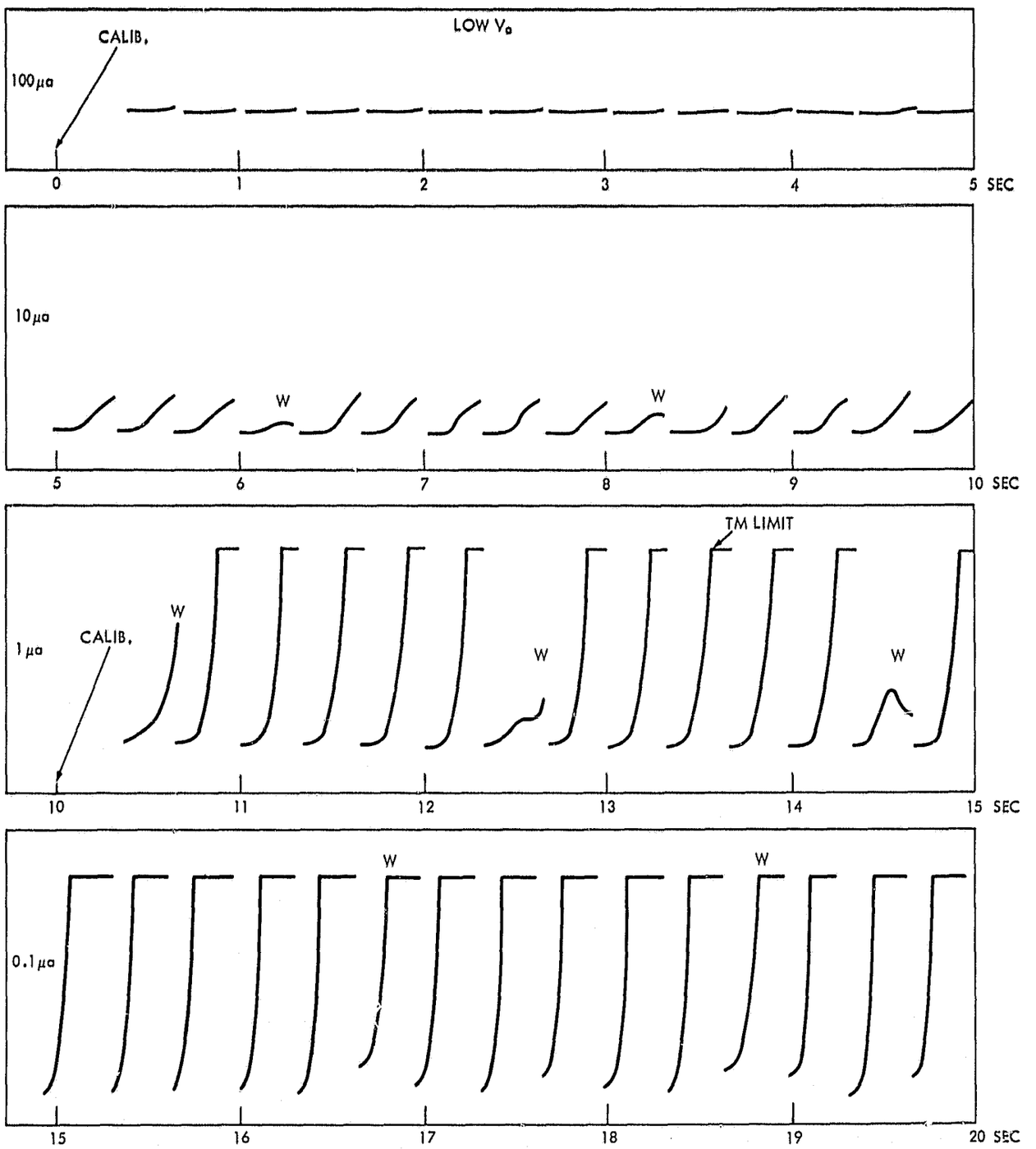

Figure 4. Analog tracing of data from a low V_a sequence immediately following the sequence shown in Figure 3.

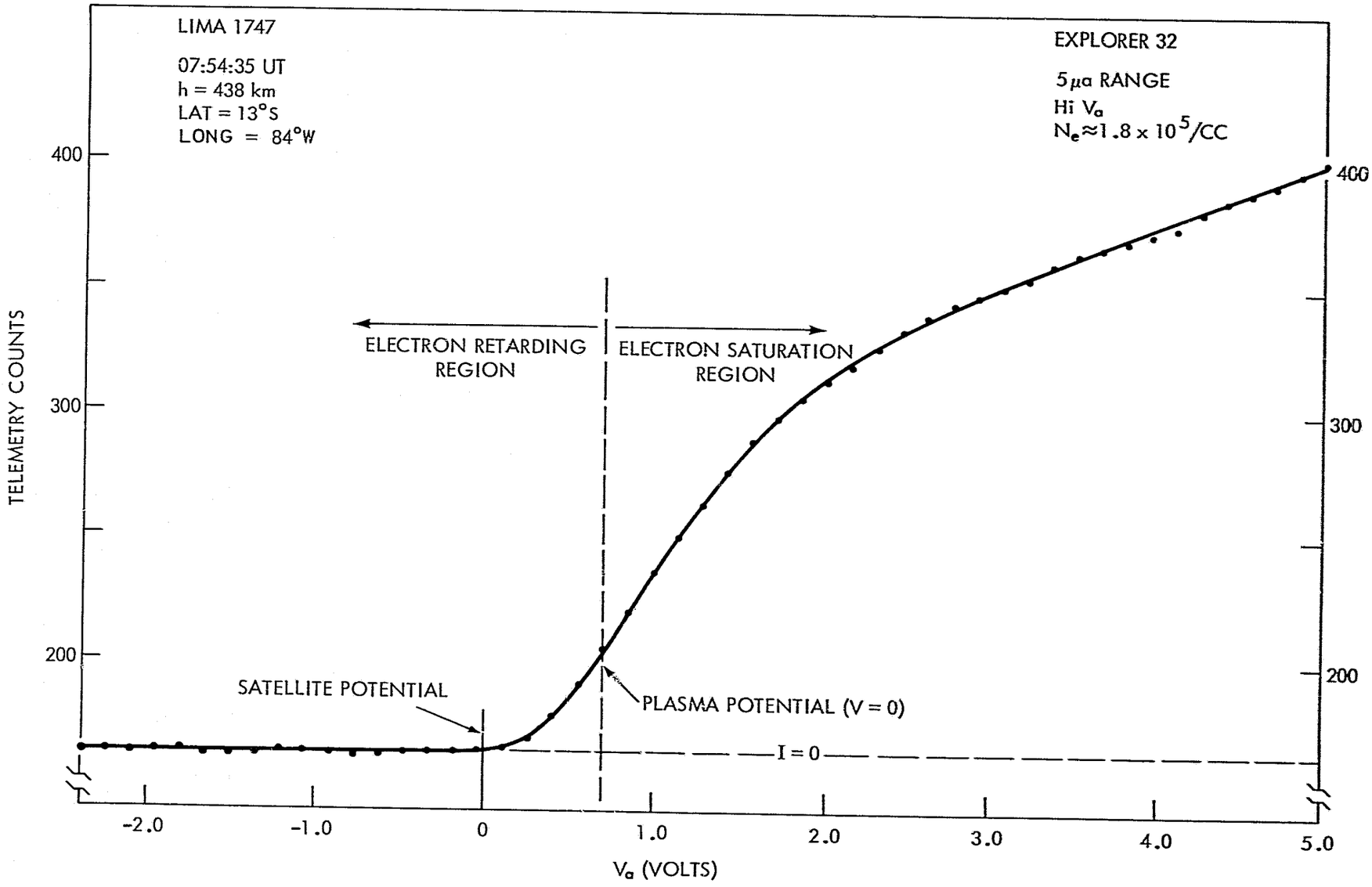

Figure 5. Full volt-ampere characteristics shows the retarding and saturation regions on a typical pass. The points are the telemetered telemetry counts, and the line is a free-hand fit to the points.

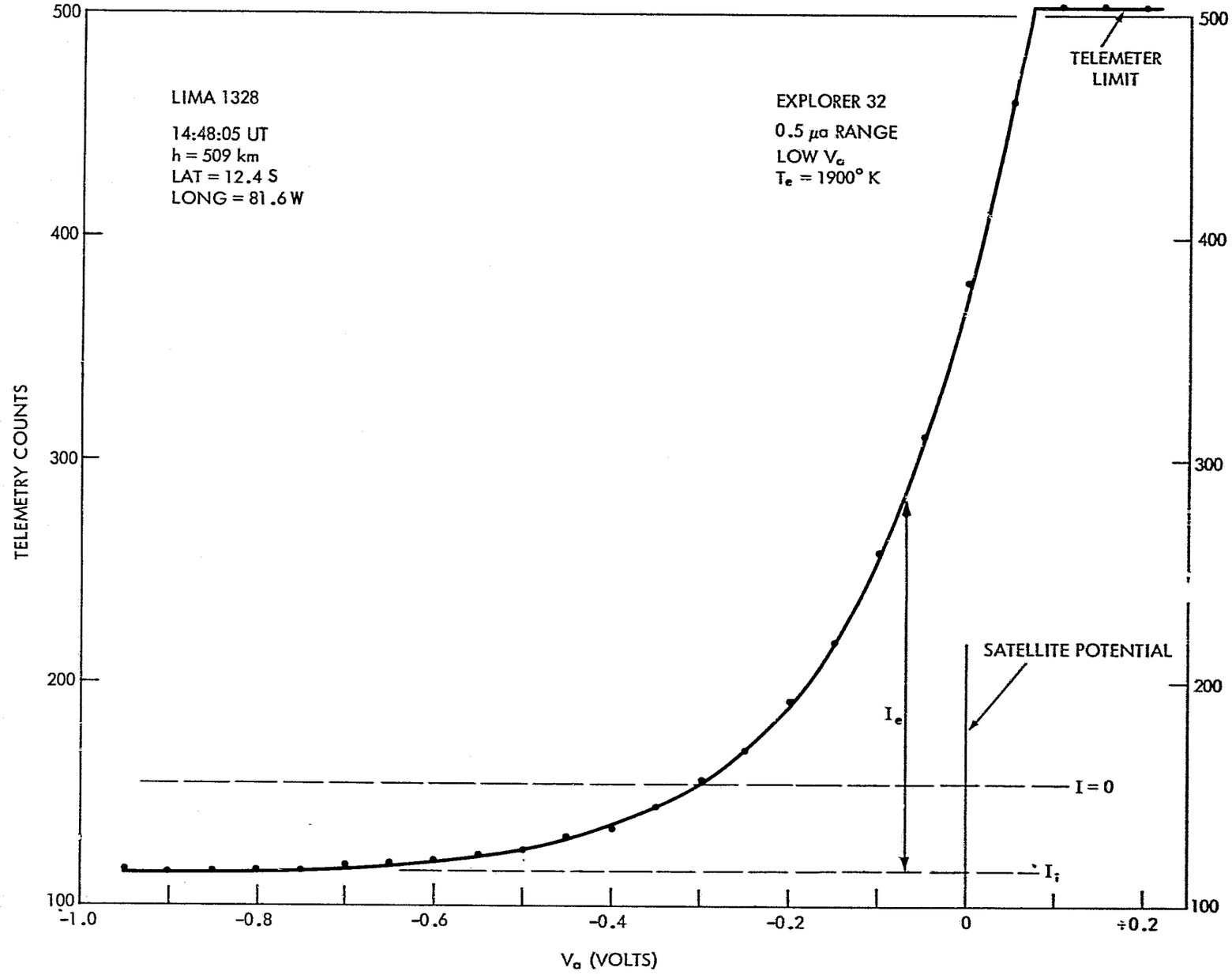

Figure 6. A retarding region taken on low V_a. The ion current (I_i) represents a downward deflection from zero current (I = 0). The electron current (I_e) rises exponentially from the ion current level.

Raw Telemetry Data

Figures 7 and 8 are plots of raw telemetry data which are presented as typical examples of the nature of the experimental output which is employed for T_e. The current range employed resolves only the electron retardation region, and a full sequence of 14 curves is shown for both high V_a (Figure 7) and low V_a (Figure 8). Curve number 1, the inflight calibration waveform, is not shown. The consecutive curves are drawn overlapping in time to compress the entire 5-second sequence onto a single plot. The zero current level is identified by a dashed line. As in Figure 6, an upward deflection from this level represents a net electron current while a downward deflection represents a net ion current. Additional ion region points have been omitted to reduce overlapping of the curves.

The effect of the wake is clearly visible in every sixth or seventh curve. These curves are easily identified and are rejected in any T_e analysis. The remaining curves taken at other orientations are essentially identical except for the level of ion current, which is also attitude dependent (Brace et al., 1965a) (Bettinger, 1967). Maximum ion currents occur when the probe axis passes normal to the direction of motion and thus presents its full cross sectional area to the ion stream. The ion current is greatly reduced in the wake and is somewhat reduced when the probe is pointed generally forward.

From Figures 7 and 8, it is clear that the voltage resolution on high V_a, although adequate for deriving T_e in this example, is not as good as that available on the low V_a. Conversely, the high V_a curves have the advantage that the retarding region is resolved in one third the time (in this case 30 milliseconds instead of 90 milliseconds) and are therefore less likely to be distorted by time-related variations within the sweep.

The $\ell n\ I_e$ Plots

As mentioned earlier, the temperatures are derived from log plots of the electron retardation currents from characteristics such as shown in Figure 7 and 8. The ion current level and slope are measured as demonstrated in Figure 6, and the electron current characteristic is taken as the difference between the measured current and the extrapolated ion current. If the electron energy distribution is Maxwellian, the plot of $\ell n\ I_e$ vs V will be linear over several decades of current. In practice, when a linear current detection system is employed, telemetry accuracy limits the current resolution to about two decades within a single curve.

Figures 9 through 13 show the log plots which are the basis for the temperatures employed in the comparisons. The error bars on the individual points represent typical telemetry error (± 1 count) which becomes negligible as the

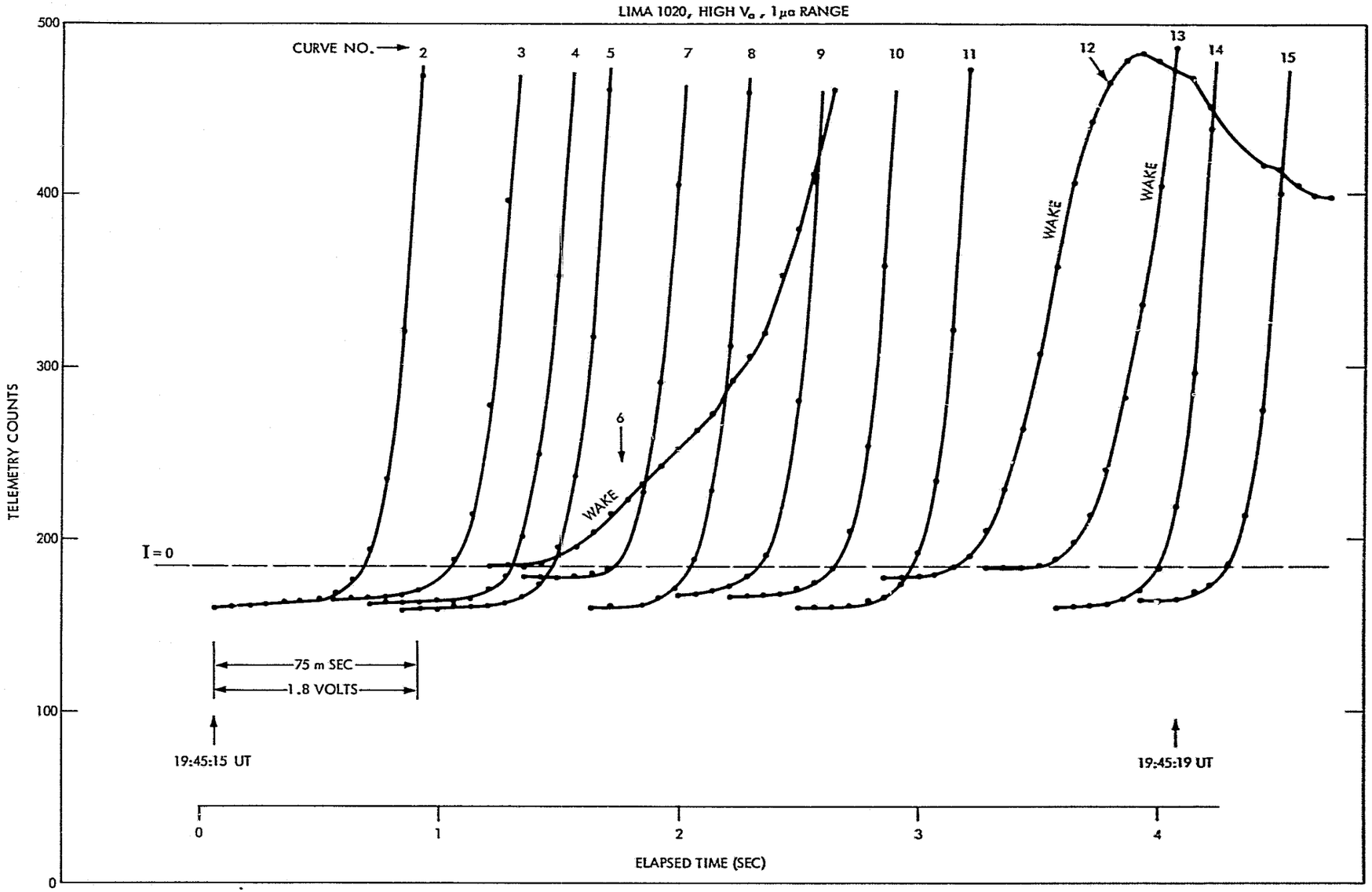

Figure 7. Raw telemetry data points on high V_a (150 mv sampling interval) showing a full sequence of retarding region electron currents. This sequence of curves were recorded in a 5-second interval, but are overlapped in time on this plot to compress them onto a single figure. Curves 6, 12 and 13 are distorted by wake effects in both the ion and electron current regions. The other curves are nearly identical in shape and the temperatures derived from each would agree well.

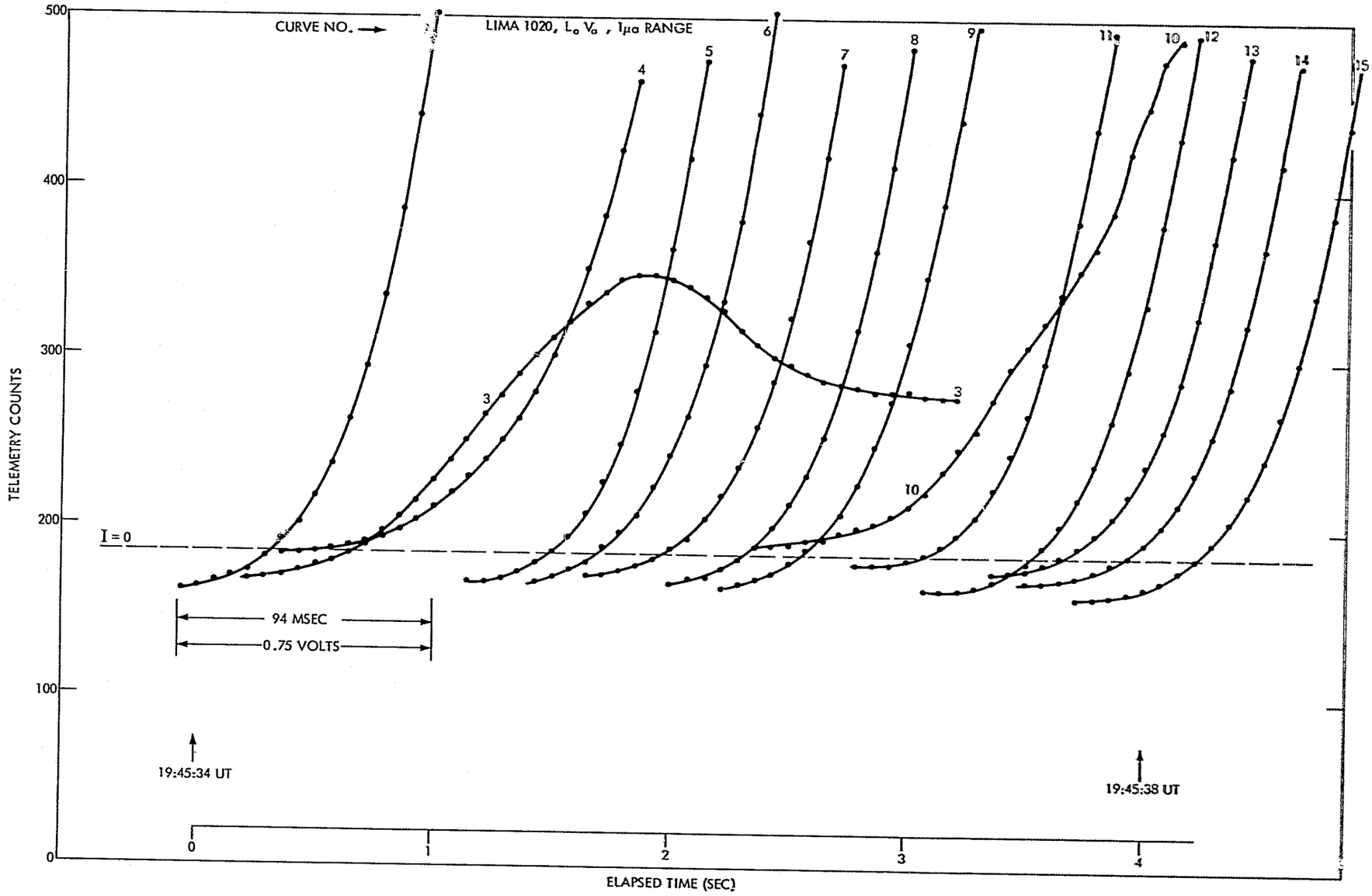

Figure 8. Raw telemetry data points on low V_a (50 mv sampling interval) showing a sequence of retarding currents with full voltage resolution. These curves were recorded about 20 seconds after the high V_a curves shown in Figure 7. Wake curves 3, 4 and 10 are easily identified.

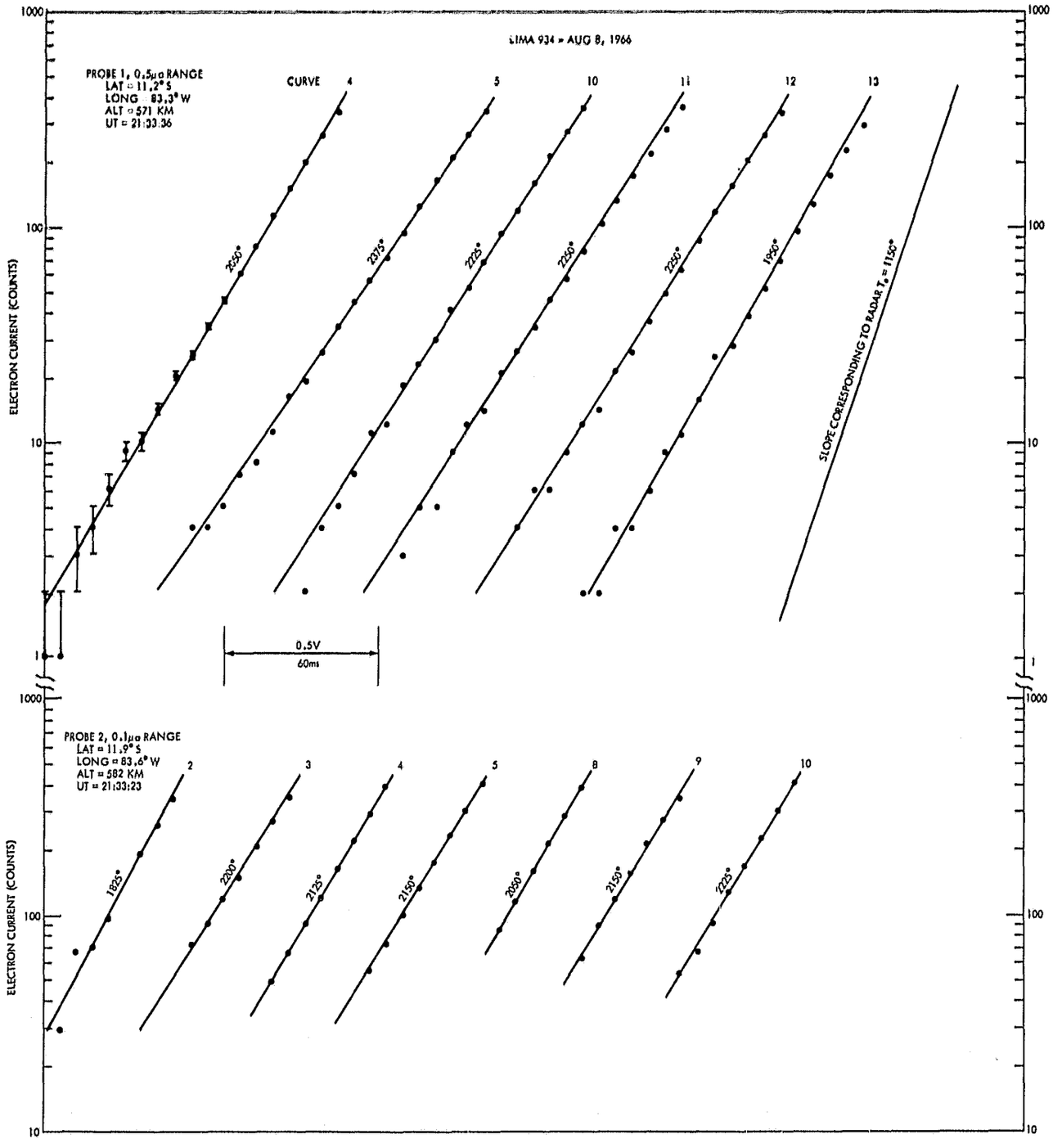

Figure 9. Log plots of the non-wake curves from the first comparison pass LIMA 934. Probe 1 and Probe 2 curves, taken about 13 seconds apart, agree well within the scatter of the values. The slope corresponding to the radar value (T_e = 1150°) is shown for comparison. The error bars on the initial curve represent the telemetry error (±1 count).

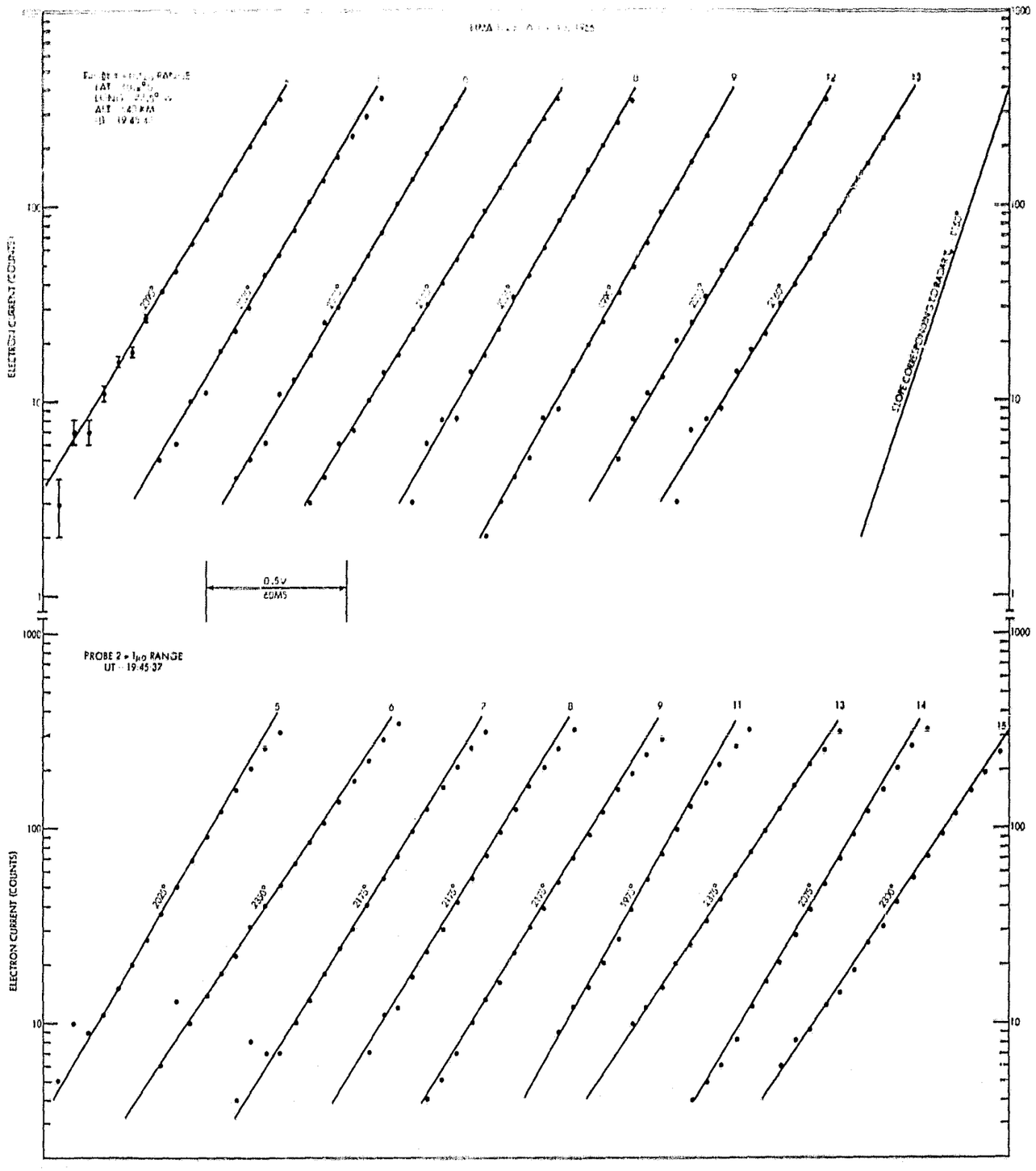

Figure 10. Log plots of curves taken on LIMA 1020, the second comparison pass in Table I. The two probes agree well. The scatter of the values is less than 10% from the average value. The slope corresponding to the radar temperature (1150°K) is much greater.

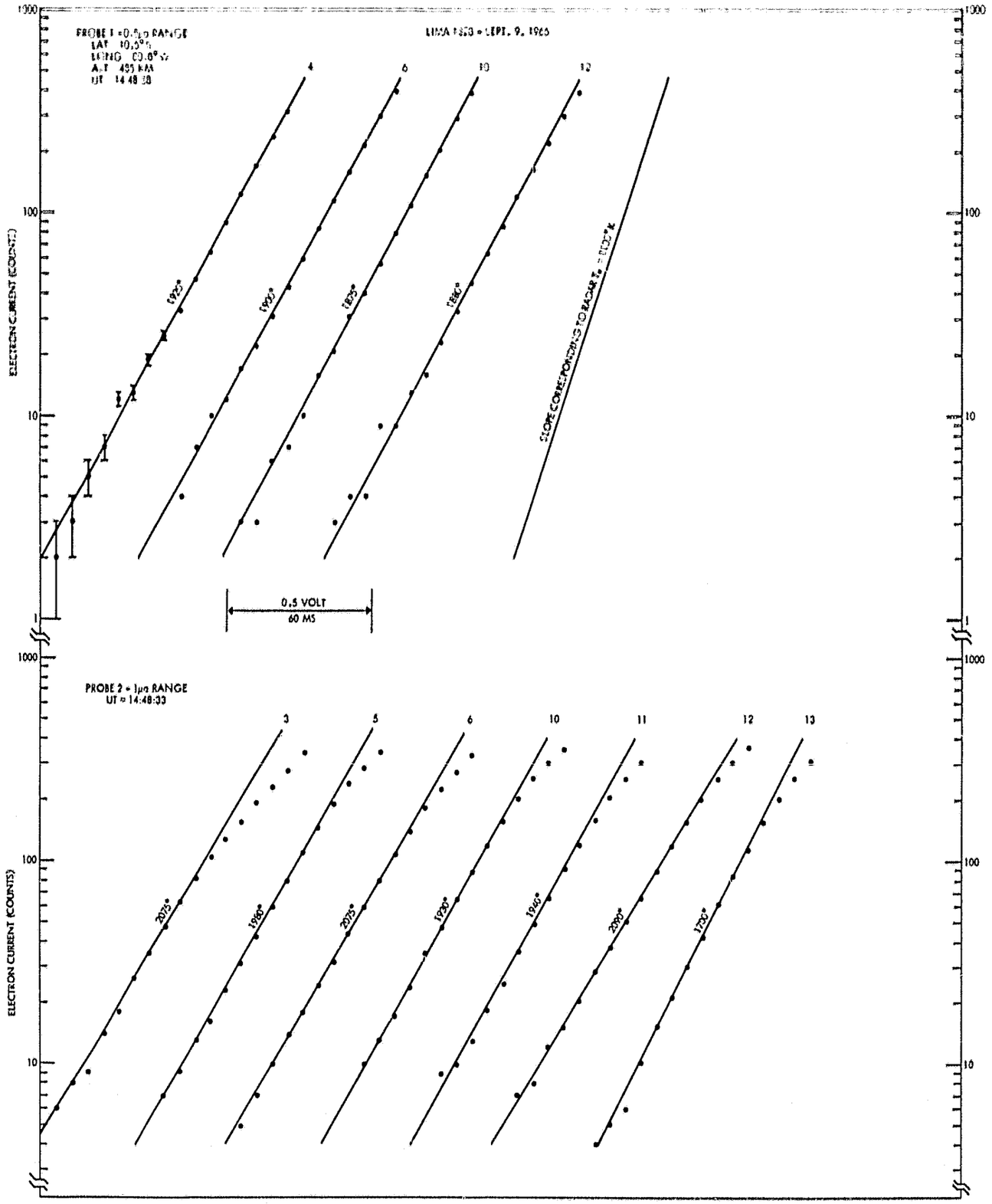

Figure 11. Log plots of curves taken on LIMA 1328, the third comparison pass.

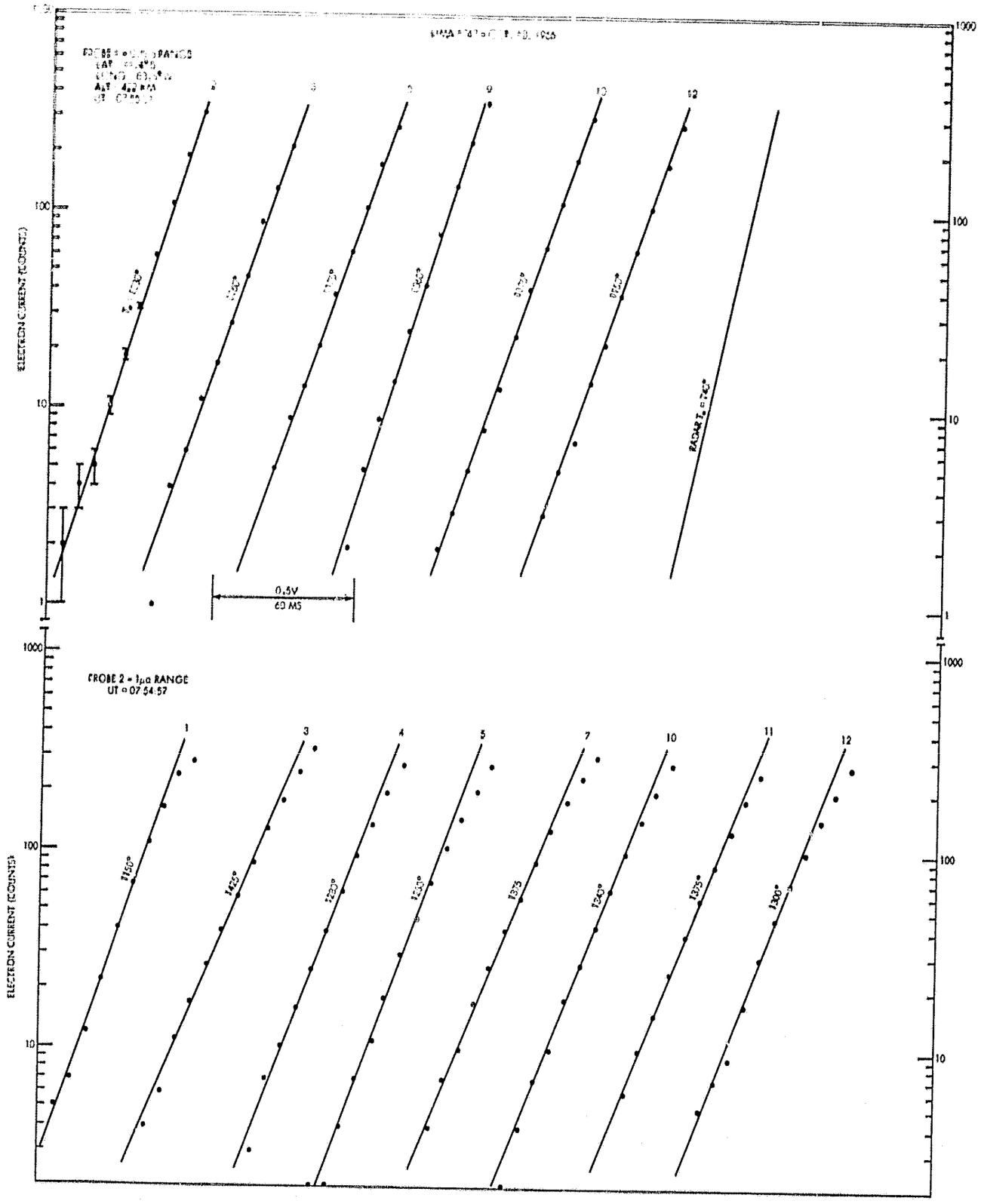

Figure 12. Log plots of curves taken on LIMA 1747, the fourth comparison pass.

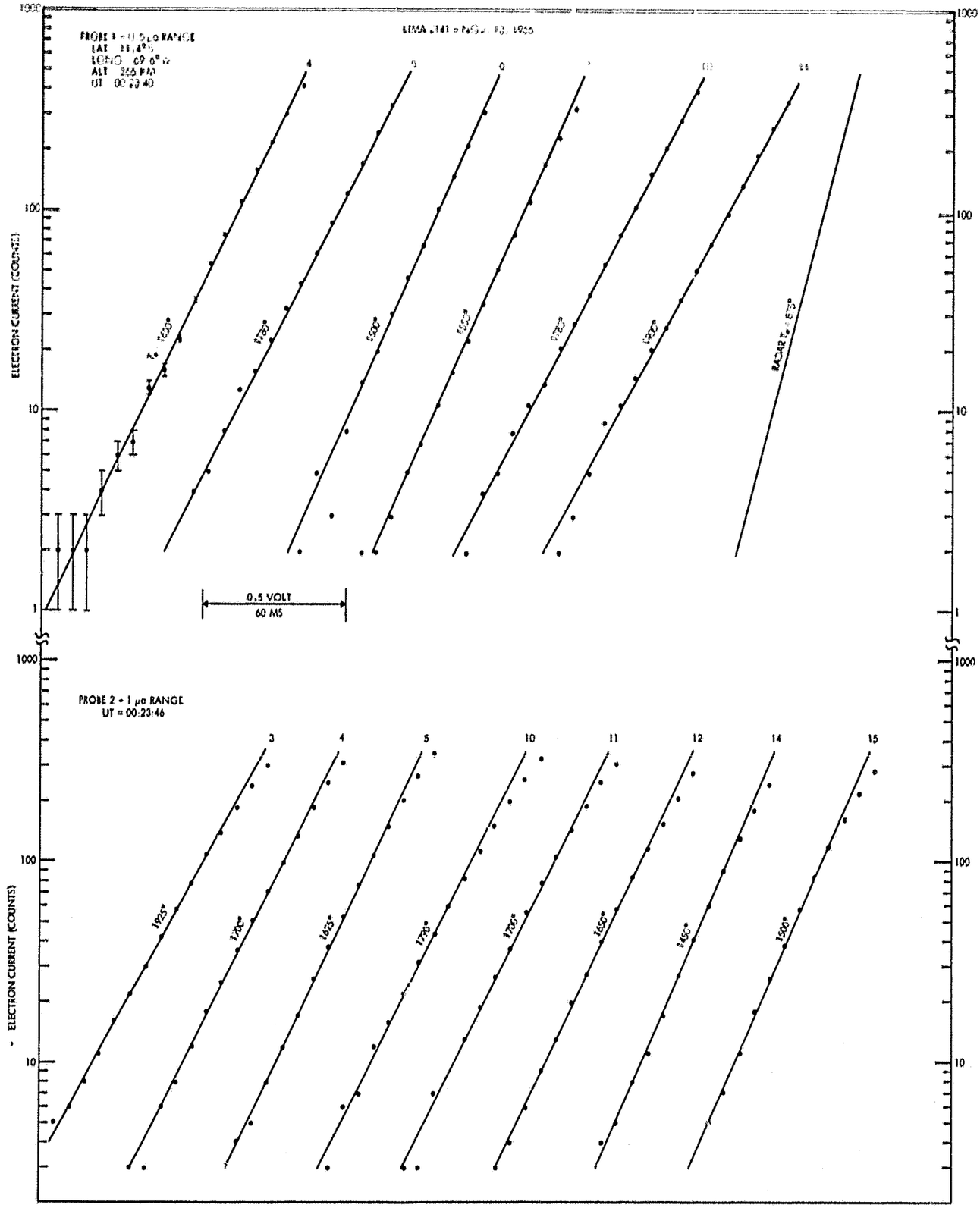

Figure 13. Log plots of curves taken on LIMA 2141, the fifth comparison pass.

current approaches full scale. In some of these passes, the plasma potential remains on-scale on the 1 μa range. This is evident as the upper points fall below the linear region defined by the lower points. For purposes of comparison we have included in each figure a theoretical $\ell n\ I_e$ line corresponding to the much lower temperatures derived from the radar measurements.

The mean temperatures from the two probes agreed within 5% in all but one pass, LIMA 1747, in which a 15% difference was observed. This is an unusually large difference from our experience and the reasons for it have not been satisfactorily explained. Perhaps the chance rejection of individual curves biased one or both mean temperatures. The two sets of data are not actually simultaneous, thus it remains possible that horizontal gradients are responsible for the difference.

DISCUSSION OF ERRORS

As in most experimental studies, the validity of the results can be judged in part by the internal consistency between the experimental data and the theory employed to interpret the data. For the measurement of T_e by probes, the prime criterion is the firm identification of an exponential retarding region. This reduces to demonstrating a well defined linear region in the $\ell n\ I_e$ plot. It is also necessary to demonstrate that temperatures derived from each sequence of curves exhibit a reasonable degree of consistency. In addition, where two independent simultaneous measurements are performed, these should also agree. The log plots of Figures 9-13 meet all three of these requirements reasonably well.

In the following paragraphs the sources of random and systematic error in T_e are discussed in detail.

Random Errors

The electron temperatures derived from individual curves within a 5-second sequence usually fall within 10% of the mean temperature. The following factors are probably the prime causes of the apparently random variation within these limits.

1. Real structure in the ionospheric temperature or concentration along the the 40-kilometer path traversed in a range sequence (15 curves).

2. Slight wake effects within some of the curves which are not badly enough distorted to be rejected initially as wake curves.

3. Anisotropy of the electron velocity distribution related to temperature gradients along the geomagnetic field tubes. For example, an upward pointed probe tends to collect electrons which suffered their last

thermalizing collisions at higher altitudes where T_e is usually greater. The spinning motion of the satellite should modulate this effect at the spin rate, if it is detectable.

4. Other second order effects which may change the current or voltage within the time of a single retarding sweep. An example of this is the voltage induced in the satellite as it moves through the geomagnetic field. The d.c. value of the induced voltage is unimportant, but its rate of change on a rapidly spinning satellite can be a significant fraction of the dV_a/dt of the sweep. At high latitudes, where the field strength is greatest and the satellite motion is nearly normal to the field, this voltage can modify dV/dt by 2% on high V_a and 6% on low V_a. However, this effect is essentially undetectable at the equator where the field is weaker and the satellite moves nearly parallel to the field.

Systematic Errors

Two sources of systematic error are of enough significance to warrant discussion, both of them relating to the question of how much of the applied voltage actually reaches the collector. The applied voltage waveform is linear and its amplitude is constant to within 1%. Its value is monitored during the measurements. However, some of the applied voltage is dropped in the internal resistance of the measurement circuits and some is lost in changing the potential of the reference.

The voltage drop within the circuits can be calculated readily since the internal resistances (R) and the current (I) are known. Since the current waveform is nonlinear, the $I \cdot R$ correction is also nonlinear, being most significant near the plasma potential where the impedance of the probe-plasma combination is lowest. This tends to make the high currents fall off the log plot prematurely and permits a slightly higher temperature line to be fitted to the entire set of points. The amount of error introduced depends upon the temperature and the detector employed, however experience indicates that the average correction for the $I \cdot R$ drop is less than 5% at the temperatures found in these comparison passes.

The second source of systematic error, the stability of the spacecraft as a potential reference, is not as easy to calculate. A good reference should have large conducting areas which are symmetrically distributed about the spin axis. Then increases in electron current collected by the probes will be balanced by decreases in electron current to the reference with negligible changes in reference potential. Ideally, the ratio of satellite to probe area should be greater than 1000:1 to achieve this.

The total area of the satellite was about 2.5×10^4 cm^2. About one third of this was in a band of bare stainless steel about the equator of the satellite.

Another one third was coated with a few-angstrom thickness of silicon monoxide needed for thermal balance. Rocket flight tests have shown that this surface remains a good conductor for thermal electrons. The remaining one third of the surface was covered with solar cells which did not contribute to the conducting area. Thus a conducting area of 1.6×10^4 cm^2 was considered a good reference area for balancing the electron current to the probes. The driven area of each probe was 16 cm^2, resulting in a reference-to-probe area ratio of about 1000:1. It can be shown that the total change in reference potential within the retarding region of a probe curve should be less than 1% of the change in probe voltage. However this change occurs nonlinearly, with the greatest rate of change in reference potential occurring as the probe reaches the plasma potential. In practice this has the same kind of effect as does the $I \times R$ drop, since it causes a slightly higher temperature to be derived from the log plots. It appears that the change in reference potential produces less than 5% increase in the derived T_e.

The correction for each of these voltage errors is nearly negligible by itself (< 5%), however both effects act in the same direction and their combined effect should not be entirely neglected in a precise comparison. For this reason we have applied an average combined correction of 5% in arriving at the tabulated values of T_e shown in Table I.

SUMMARY AND CONCLUSIONS

In this report, we have (1) outlined the theory and implementation of the probe experiments on Explorer 32, (2) shown examples of the raw telemetry data, (3) shown log plots of the electron currents from all curves used in the radar comparisons, and (4) discussed the possible sources of random and systematic error in the probe measurements as we see them. We have concluded that these sources of error cannot conceivably explain the 70% disagreement between the probe and backscatter measurements. Furthermore we are aware of no other sources of error which could produce the volt-ampere characteristics which were observed if the temperature were actually as low as the radar indicated.

ACKNOWLEDGMENT

We are grateful to George R. Carignan and Tuck B. Lee of the University of Michigan for their efforts in the design and fabrication of the electronic equipment which operated flawlessly throughout the satellite lifetime. We also thank Larry Rudolph for the computer program which made the data available in a form convenient for analysis.

REFERENCES

Betlinger, R. T. "An End Effect Associated With Cylindrical Langmuir Probes Moving at Satellite Velocities" Transactions of the AGU; 48, 86, (1967)

Brace, L. H., N. W. Spencer, A. Dalgarno, "Detailed Behavior of the Midlatitude Ionosphere from the Explorer 17 Satellite" Planet. Space Sci., 13, 647, (1965a)

Brace, L. H., B. M. Reddy, "Early Electrostatic Probe Results From Explorer 22" J. Geophys. Res., 70, 5783, (1965b)

Brace, L. H., B. M. Reddy, H. G. Mayr "Global Behavior of the Ionosphere at 1000-Kilometer Altitude", J. Geophys. Res., 72, 265, (1967)

Brace, L. H. and J. A. Findlay, "Comparison of Cylindrical Electrostatic Probe Measurements of Alouette-II and Explorer 31 Satellites" (Special Issue IEEE, Accepted for Publication, 1968)

Findlay, J. A., L. H. Brace, "Cylindrical Electrostatic Probes Employed on Alouette-II and Explorer 31 Satellites" (Special Issue of IEEE, Accepted for Publication, 1968)

Hanson, W. B., L. H. Brace, P. L. Dyson and J. P. McClure "Conflicting Electron Temperature Measurements in the Upper F-Region" (Submitted to J. Geophys. Res.), 1968

Mott-Smith, H. M., and I. Langmuir "The Theory of Collectors in Gaseous Discharges, Phys., Rev., 28, 727, 1926

Reddy, B. M., L. H. Brace, J. A. Findlay, "The Ionosphere at 640 Kilometers on Quiet and Disturbed Days." J. Geophys. Res., 72, 2709, (1967)

Spencer, N. W., L. H. Brace, and G. R. Carignan, "Electron Temperature Evidence for Nonthermal Equilibrium in the Ionosphere" J. Geophys. Res., 67, 157, (1962)

Spencer, N. W., L. H. Brace, G. R. Carignan, D. R. Taeusch and H. Niemann "Electron and Molecular Nitrogen Temperature and Density in the Thermosphere" J. Geophys. Res., 70, 2665, (1965)